MedChemComm

The official journal of the European Federation for Medicinal Chemistry

Accepted Manuscript

This article can be cited before page numbers have been issued, to do this please use: A. R. Santos, H. M. Sheldrake, A. Ibrahim, C. Danta, D. Bonanni, M. Daga, S. Oliaro-Bosso, D. boschi, M. L. L. LOLLI and K. Pors, *Med. Chem. Commun.*, 2019, DOI: 10.1039/C9MD00201D.

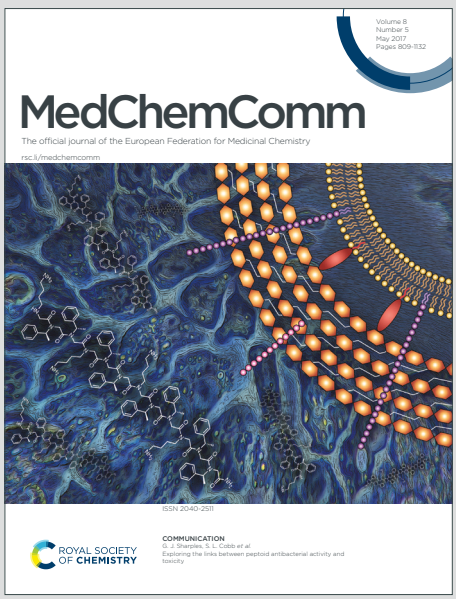

ROYAL SOCIETY OF CHEMISTRY

rsc.li/medchemcomm

View Article Online
DOI: 10.1039/C9MD00201D

ARTICLE

Exploration of [2+2+2] cyclotrimerisation methodology to prepare tetrahydroisoquinoline-based compounds with potential aldo-keto reductase 1C3 target affinity

Received 00th January 20xx,
Accepted 00th January 20xx

DOI: 10.1039/x0xx00000x

Ana R. N. Santos,[a] Helen M. Sheldrake,[a] Ali I.M. Ibrahim,[a,b] Chhanda Charan Danta,[a] Davide Bonanni,[c] Martina Daga, Simonetta Oliaro-Bosso,[c] Donatella Boschi,[c] Marco L. Lolli[c] and Klaus Pors[a,*]

Tetrahydroisoquinoline (THIQ) is a key structural component in many biologically active molecules including natural products and synthetic pharmaceuticals. Here, we report on the use of transition-metal mediated [2+2+2] cyclotrimerisation of alkynes to generate tricyclic THIQs with potential to selectively inhibit AKR1C3.

1. Introduction

Prostate cancer is the most commonly diagnosed cancer and the second leading cause of death in men.[1] Patients that no longer respond to radiation and androgen deprivation therapy (ADT) develop castration-resistant prostate cancer (CRPC), which is a lethal disease with no curative treatment options. In the steroid biosynthesis pathway, the aldo-keto reductase family 1 member C3 (AKR1C3) is an enzyme that is known to catalyse transformation of the hormone precursors androstenedione and androsterone to highly active testosterone and dihydrotestosterone (DHT) respectively, which is linked with prostate cancer cell proliferation.[2] Much AKR1C3 inhibitor research has been focused on medroxyprogesterone acetate (MPA), steroidal lactones, cinnamic acids, flavonoids and nonsteroidal anti - inflammatory drugs (NSAIDs)[3] while new potent and selective 1,3,5-metasubstituted retroinverted amides show promise for *lead* optimisation.[4] Our interest in novel drug design approaches[5-7] has recently led to the discovery of benzoisoxazole, hydroxytriazole and hydroxyfurazan NSAIDs as potent and selective AKR1C3 inhibitors by application of a bioisosteric scaffold hopping approach.[8-11]

Tetrahydroisoquinoline (THIQ) is a key structural component of many biologically active natural products and synthetic derivatives. As a consequence, THIQ has been used as a strategic building block for both synthetic explorations and for the generation of small molecules of biological interest.[12-16] Recently, Pictet-Spengler chemistry and *in silico* studies were employed to generate a novel series of THIQ-triazole based analogues, which showed AKR1C3 to be a plausible target.[17] Interestingly, [2+2+2] cyclotrimerisation methodology have been exploited to generate functionalised phosphorus analogues of the THIQ pharmacophore[18] and fused indoloisoquinolines[19] from diyne and terminal alkyne intermediates. Indeed, [2+2+2] cyclotrimerisations have been shown to be useful in the synthesis of a variety of molecular structures ranging from intricate natural products to synthetically interesting small molecules.[20] Here we report on the synthesis of tricyclic THIQs using a transition-metal mediated [2+2+2] cyclotrimerisation strategy to generate novel compounds to target AKR1C3.

2. Results and discussion

2.1 Chemical explorations

Dialkyne **9** was prepared starting from **4** in three steps (Scheme 1A). Racemic alkyne **7** was obtained by the reaction of allenyltributylstannane **6** with ethoxylactams **5**.[21] Dialkyne **9** was obtained by treatment of **7** with NaH and propargyl bromide in 83 % yield.

The transition metal-mediated [2+2+2] cyclotrimerisation of alkynes was investigated initially using dialkyne **9**, Wilkinson's catalyst ($Rh(PPh_3)_3Cl$, 5 mol %) and diethyl acetylenedicarboxylate **10a** ('a' denotes specific alkyne used, see Table 2), in refluxing toluene. The desired tricyclic product **14a** was obtained in 30 % yield along with the hexasubstituted benzene **11a** resulting from trimerisation of monoalkyne **10a** (24 %), and pentasubstituted benzenes **12a** (21 %) and **13a** (22 %), which resulted from the intermolecular reaction of two molecules of monoalkyne **10a** and the individual alkyne branches of dialkyne **9** (Scheme 1B). The optimisation of this reaction is further reported in Table S1.

Next, we decided to investigate the influence of the catalyst on the product formation. Encouragingly, the yield of **14a** could be increased to 70 % with Cp*Ru(cod)Cl as the catalyst (entry 4, Table 1), indicating this was the most chemoselective of the four catalysts used.

[a] *Institute of Cancer Therapeutics, Faculty of Life Sciences, University of Bradford, West Yorkshire, BD7 1DP, UK..*
[b] *Present address: Department of Pharmacy, Al-Zaytoonah University of Jordan, Queen Alia Airport St 594, Amman, 11733, Jordan.*
[c] *Department of Science and Drug Technology, University of Torino, Via Pietro Giuria 9, 10125 Torino, Italy.*
* Corresponding Author; Email: k.pors1@bradford.ac.uk
Electronic Supplementary Information (ESI) available: Synthetic protocols, [2+2+2] cyclotrimerisation optimisation and binding mode of **14a** in AKR1C2. protocols.. See DOI: 10.1039/x0xx00000x

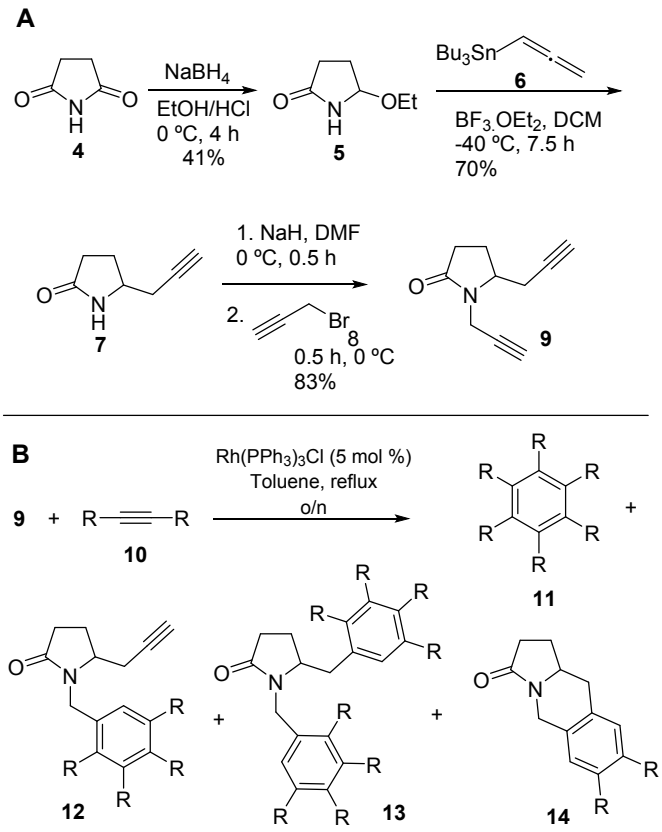

Scheme 1. Synthesis of key dialkyne 9 (A) and THIQ analysis of by-products (B). See Table 2 for identity of R groups used.

Table 1. Exploration of catalysts to faciliate [2+2+2] cyclotrimerisation of dialkynes.

Entry	Catalyst	Time (h)	Yield (%)			
			11a[c]	**12a**	**13a**	**14a**
1	$Rh(PPh_3)_3Cl$[a]	18	24	21	22	30
2	$CpCo(CO)_2$[b]	4	11	3	7	44
3	$[Ir(cod)Cl]_2$ [b, d]	6.5	32	18	7	18
4	Cp*Ru(cod)Cl[b]	2.5	12	trace	10	70

Catalysts tested for the synthesis of tricyclic adduct **14a**. Reactions performed with 0.310 mmol of dialkyne **9**, 5 eq. of diethyl acetylenedicarboxylate **10a** in refluxing toluene (2 mL). [a]5 mol % catalyst, [b]10 mol % catalyst, [c]yield based on the amount of diethyl acetylenedicarboxylate **10a** used, [d]DIPHOS 10 mol %.

2.2 Biological evalution and computational analysis

The 2,3-functionalised THIQ **14a** and a small panel of analogues (**14e**, **15**-**18**) with modified electronic properties, which could be easily synthesised from **14a**, were subjected to AKR1C3 molecular docking studies using GLIDE Induced Fit protocol[22] in order to identify possible binding affinities. Calculated binding energies for both the carboxyethyl (**14a**, -11.76 kcal/mol) and carboxylic (**15**, 12.40 kcal/mol) THIQs were shown to be comparable with berberine (-11.56 kcal/mol), an isoquinoline alkaloid and known AKR1C3 inhibitor.[23] However, compound **14e** showed a slightly lower docking score (-10.61 kcal/mol) to berberine while compounds **16**-**18** had at least two orders of magnitude smaller docking score than berberine (Figure 1). Accordingly, only compounds **14a**, **14e** and **15** were synthesised and selected for *in vitro* screening using AKR1C2 and 1C3 purified enzymes. Starting from compound **14a**, the carboxylic acid **15** and the hydroxymethyl analogue **14e** were obtained by either acidic hydrolysis or reductive conditions (see ESI).

Table 2. Exploration of alkynes suitable for [2+2+2] cyclotrimerisation chemistry.

Entry	Mono alkyne	R =	Time (h)	Yield (%)			
				11a	**12**	**13**	**14**
1	(**10a**)	EtO_2C	2.5	12	trace	10	70
2	(**10b**)	MeO_2C	1	22	---	17	34
3	(**10c**)	CH_3CH_2	20	Degraded			
4	(**10d**)	$CH_3(CH_2)_2$	20	Degraded			
5	(**10e**)	CH_2OH	4 days	Degraded			
6	(**10e**)	CH_2OH	3 days[b]	Degraded			
7	(**10f**)	CH_2Cl	24	Degraded			
8	(**10g**)	C_6H_5	24	32	---	---	trace
9	(**10h**)	TMS	24	Degraded			

Reactions performed with 0.310 mmol of dialkyne **9**, 5 eq. of monoalkyne **10** in 2 mL of toluene under reflux with 10 mol % of Cp*Ru(cod)Cl. [a]yield based on the amount of monoalkyne used, [b]reaction carried out in DMF at 110 ºC.

Compounds **14a**, **14e** and **15** were assayed at up 50 µM and inhibitory effect was observed for all compounds against AKR1C3 (Table 3). Berberine was found to be the most potent compound, but did not exhibit AKR isoform selectivity. In contrast, **14a** was 8-fold more potent in inhibiting AKR1C3 over 1C2. Given the lower potency in inhibiting **14e** and **15** these compounds were not assayed against AKR1C2.

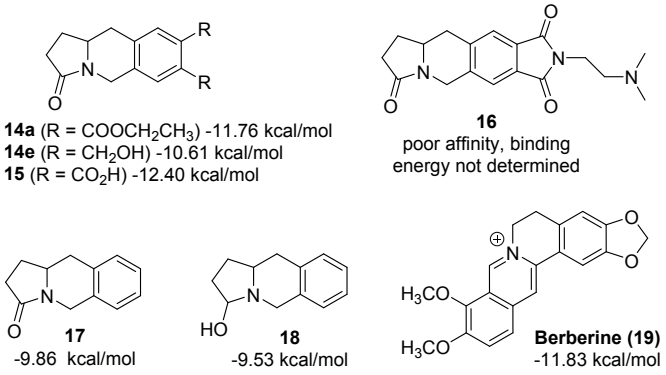

Fig. 1. 2,3-hybridised THIQs with calculated binding energies from AKR1C3 molecular docking studies using GLIDE.

Subsequently, we analyzed the predicted binding mode of **14a** (Figure 2). The compound was shown to extend into sub-pocket 3 (SP3) (Tyr24, Glu192, Ser217, Ser221, Gln222, Tyr305, Phe306),[24] and link an H-bond into oxyanion site (OS) with Tyr55 and His117.

Furthermore, **14a** shows a π-π stacking interaction with the Phe306 residue while still being able to protrude inside both SP1 (Ser118, Asn167, Phe306, Phe311, Tyr319) and SP2 (Trp86, Ser129, Trp227, Phe311) binding pockets with the ester groups and enabling H-bond interaction with Ser118. Whilst berberine was not selective over AKR1C2, **14a** demonstrated encouraging selectivity that can

possibly be correlated with the more restricted AKR1C2 binding pocket compared with AKR1C3.[24]

Table 3. Inhibitory effect on AKR1C3 and AKR1C2 recombinant enzymes.

Compound	AKR1C3 inhibition[a] IC_{50} (µM) ± SE	AKR1C2 inhibition IC_{50} (µM) ± SE
Berberine	5.90 ± 0.19	6.71 ± 2.17
14a	11.69 ± 0.41	96.20 ± 7.17
14e	> 50 (25.04 % ± 3.95)[b]	> 50 (26.90 % ± 1.56)[b]
15	23.11 ± 1.85	27.33 ± 4.34

[a] Experiments performed with *S*-tetralol as substrate, [b] % of inhibition ± SE at 50 µM.

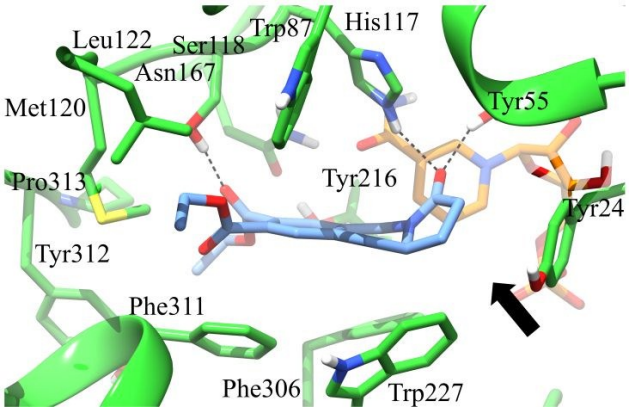

Fig. 2. Compound **14a** docking pose in the AKR1C3 binding site. Dash lines represent H-bond, the bold arrow indicates sub-pocket 3. Only the most significant amino acids are shown.

To better investigate this hypothesis, a docking analysis of compound **14a** on AKR1C2 was conducted (Figure S3). Because of the tighter binding pocket, compound **14a** was found unable to interact with SP1 and presented a completely different binding mode in comparison with AKR1C3 illustrated above. The reduced affinity for AKR1C2 is in agreement with a lower predicted binding energy (-10.31 kcal/mol), indicating a non-optimal protein-ligand interaction. Clearly, while further investigations are necessary to fully understand the therapeutic potential of THIQs, the data presented here suggest a useful starting point for design of more potent and selective AKR1C3 inhibitors.

Conclusions

In summary, dialkyne, **9** was prepared using amide reduction and aminal substitution to introduce one propargyl sidechain, followed by amide N-alkylation with propargyl bromide to introduce the second chain. A transition-metal catalysed [2+2+2] cyclotrimerisation of a pyrrolidinone dialkyne was then used as a new approach to synthesise 2,3-functionalised THIQ derivatives. The best yield resulted from the reaction of dialkynes **9** with diethylacetylene dicarboxylate **10a** and Cp*Ru(cod)Cl in refluxing toluene. This approach allows the aromatic part of the molecule to be assembled at a late stage of the synthesis. An advantage of diversifying the THIQ pharmacophore at this late point is that the substituents around the aromatic ring of the THIQ can be introduced with relative ease, providing libraries of new small molecules with improved potency and selectivity for AKR1C3.

Experimental

Chemical synthesis

The detailed experimental procedures for all new compounds can be found in the ESI.

Computational modelling

The structures of compounds **14** - **18**, as well as the structure of berberine, were constructed using the 2D Sketcher tool implemented in Maestro GUI. For each compound, an advanced conformational search was performed using OPLS_2005 as Force Field and setting 1000 maximum steps for each run. Molecular docking was performed using Schrodinger Induced Fit Docking protocol (IFD).[22] For this purpose, the X-ray crystallographic structure of AKR1C3 was retrieved from RCSB Database (PDB code: 1S2C)[25] and the generated conformers were docked. Before docking, the crystal structure of the protein underwent an optimisation process using the Protein Preparation Wizard tool, implemented in Maestro™ GUI. Missing hydrogen atoms were added and bond orders were assigned. Then, DMS, non-structural water molecules and impurities (such as solvent molecules) were removed. Cofactor Acid NAP was maintained. Reorientation of automatically optimised hydrogen bond network: hydroxyl and thiol groups, amide groups of asparagine (Asn) and glutamine (Gln), and the imidazole ring in histidine (His). Moreover, the prediction of protonation states of His - aspartic acid (Asp), glutamic acid (Glu), and tautomeric states of His – were accomplished using PROPKA™. Standard IFD protocol was performed using the co-crystallised ligand flufenamic acid to center the grid. Protein preparation constrained refinement and Glide XP re-docking were settled, the other parameters were kept by default.

Expression and purification of recombinant human AKR1C3 and AKR1C2

Escherichia coli BL21 (DE) Codon Plus RP cells expressing recombinant AKR1C3 and AKR1C2 proteins were used. Protein expression and purification were performed as previously described.[8] Briefly, bacteria cells were grown in YT2X media supplemented with ampicillin at 37°C and at OD600 nm = 0.6 the expression was induced by IPTG (0.5 mM) at 24°C for 2 h. Then, bacteria were centrifuges and lysed with four freeze-thaw cycles in presence of lysozyme and protease inhibitors. DNA was digested with benzonase (25 U) in presence of $MgCl_2$ 5 mM. The lysate was centrifuged for 30 min at 13,000 x g and the supernatant was collected. AKR1C3 and AKR1C2 were affinity purified via N-terminal GST-tag on glutathione (GT) sepharose (GE-Healthcare) and cleaved of by thrombin according to the manufacturer's protocol. Expression and purification was monitored by SDS-PAGE.

In vitro AKR1C3 and AKR1C2 inhibition assays

The inhibition assays were performed on purified recombinant enzymes as previously described.[8] Briefly, the enzymatic reaction was fluorimetrically (ex/em; 340 nm/ 460 nm) monitored by the measurement of NADPH production on an "Ensight" plate reader (Perkin Elmer) at 37°C. Assay mixture contained *S*-tetralol (in EtOH), inhibitor (in EtOH), 100 mM phosphate buffer, pH 7, 200 µM $NADP^+$, and purified recombinant enzyme (30 µl) in a final volume of 200 µl and 10 % EtOH was added in 96-well plate. The *S*-tetralol concentration used in the AKR1C2 and AKR1C3 inhibition assays

were 15 µM and 160 µM, respectively; the same as the Km described for the respective isoforms under the same experimental conditions. Percent inhibition with respect to the controls containing the same amount of solvent, without inhibitor, was calculated from the initial velocities, obtained by linear regression of the progress curve, at different concentrations of the inhibitor. The IC_{50} values were obtained using PRISM 7.0, GraphPad Software. The values obtained were the means of two separate experiments each carried out in triplicate.

Conflicts of interest

There are no conflicts to declare.

Acknowledgements

This work was supported by Fundação para a Ciência, a Tecnologia (PhD studentship ARNS SFRH/BD/46871/2008), EPSRC (RCUK Academic Fellowship HMS), UniTO grant Ricerca Locale 2015 (grant number LOLM_RILO_17_01) and Fondazione Cassa di Risparmio di Torino (grant BOSD_CRT_17_2). We would like to thank Ms Teresa Folino for assistance with synthesis, Mr Andrew Healey for LRMS and the EPSRC NMSSC for HRMS measurements.

References

1. R. L. Siegel, K. D. Miller and A. Jemal, *CA Cancer J. Clin.*, 2016, **66**, 7-30.
2. A. O. Adeniji, M. Chen and T. M. Penning, *J. Steroid. Biochem. Mol. Biol.*, 2013, **137**, 136-149.
3. A. C. Pippione, D. Boschi, K. Pors, S. Oliaro-Bosso and M. L. Lolli, *J Cancer Metastasis Treat.*, 2017, **3**, 328-361.
4. K. Verma, T. Z. Zang, T. M. Penning and P. C. Trippier, *J. Med. Chem.*, 2019, **62**, 3590-3616.
5. M. Lolli, S. Narramore, C. W. G. Fishwick and K. Pors, *Drug Discov. Today*, 2015, **20**, 1018-1026.
6. K. Pors, *InTech, Drug Discovery and Development - Present and Future, Edited by Dr Izet Kapetanović*, 2011, **Chapter 4**, 69-96.
7. K. Pors, F. W. Goldberg, C. P. Leamon, A. C. Rigby, S. A. Snyder and R. A. Falconer, *Drug Discov. Today*, 2009, **14**, 1045-1050.
8. A. C. Pippione, A. Giraudo, D. Bonanni, I. M. Carnovale, E. Marini, C. Cena, A. Costale, D. Zonari, K. Pors, M. Sadiq, D. Boschi, S. Oliaro-Bosso and M. L. Lolli, *Eur. J. Med. Chem.*, 2017, **139**, 936-946.
9. M. L. Lolli, I. M. Carnovale, A. C. Pippione, W. Y. Wahlgren, D. Bonanni, E. Marini, D. Zonari, M. Gallicchio, V. Boscaro, P. Goyal, R. Friemann, B. Rolando, R. Bagnati, S. Adinolfi, S. Oliaro-Bosso and D. Boschi, *ACS Med. Chem. Lett.* 2019, **10**, 437-443.
10. A. C. Pippione, I. M. Carnovale, D. Bonanni, M. Sini, P. Goyal, E. Marini, K. Pors, S. Adinolfi, D. Zonari, C. Festuccia, W. Y. Wahlgren, R. Friemann, R. Bagnati, D. Boschi, S. Oliaro-Bosso and M. L. Lolli, *Eur. J. Med. Chem.*, 2018, **150**, 930-945.
11. S. Sainas, A. C. Pippione, A. Giraudo, K. Martina, F. Bosca, B. Rolando, A. Barge, A. Ducime, A. Federico, S. J. Grossert, R. L. White, D. Boschi and M. L. Lolli, *J. Heterocycl. Chem.*, 2019, **56**, 501-519.
12. J. D. Scott and R. M. Williams, *Chem. Rev.*, 2002, **102**, 1669-1730.
13. A. W. Kahsai, S. Zhu, D. J. Wardrop, W. S. Lane and G. Fenteany, *Chem. Biol.*, 2006, **13**, 973-983.
14. N. T. Patil, H. Wu and Y. Yamamoto, *J. Org. Chem.*, 2007, **72**, 6577-6579.
15. A. B. J. Bracca and T. S. Kaufman, *Tetrahedron*, 2004, **60**, 10575–10610.
16. Y. D. Zhou, Y. P. Kim, K. A. Mohammed, D. K. Jones, I. Muhammad, D. C. Dunbar and D. G. Nagle, *J. Nat. Prod.*, 2005, **68**, 947-950.
17. R. Pingaew, P. Mandi, C. Nantasenamat, S. Prachayasittikul, S. Ruchirawat and V. Prachayasittikul, *Eur. J. Med. Chem.*, 2014, **81**, 192-203.
18. M. A. Zotova, D. V. Vorobyeva, P. H. Dixneuf, C. Bruneau and S. N. Osipov, *Synlett*, 2013, **24**, 1517-1522.
19. A. Swami and C. V. Ramana, *Synlett*, 2015, **26**, 604-608.
20. S. Kotha, E. Brahmachary and K. Lahiri, *Eur. J. Org. Chem.*, 2005, 4741-4767.
21. W. F. J. Karstens, F. P. J. T. Rutjes and H. Hiemstra, *Tetrahedron Lett.*, 1997, **38**, 6275-6278.
22. Schrödinger Suite 2017-4, Glide, Schrödinger, 2017; Prime, Schrödinger, LLC, New York, NY.
23. Y. T. Tian, L. J. Zhao, Y. Wang, H. T. Zhang, D. Xu, X. J. Zhao, Y. Li and J. Li, *Asian J. Androl.*, 2016, **18**, 607-612.
24. M. C. Byrns, Y. Jin and T. M. Penning, *J. Steroid. Biochem. Mol. Biol.*, 2011, **125**, 95-104.
25. A. L. Lovering, J. P. Ride, C. M. Bunce, J. C. Desmond, S. M. Cummings and S. A. White, *Cancer Res.*, 2004, **64**, 1802-1810.

View Article Online
DOI: 10.1039/C9MD00201D

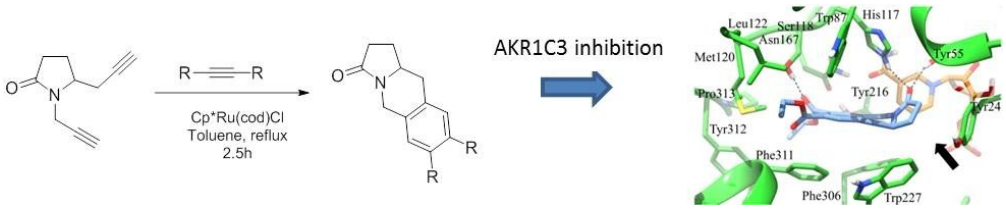

166x33mm (150 x 150 DPI)